Regular Paper

Title:

Searching for Secondary Antioxidants in Plants: Isoalliin from Onion as an Excellent Acrolein Scavenger

Running head:

Acrolein scavenging compounds in plants

Authors:

Ayako Hada [a], Chihiro Nozaki [b], Natsumi Tamura [b], Kenji Matsui [a], Yasumasa Matsuoka [c], Daisuke Shibata [d#], Jun'ichi Mano [a,e,f*†]

Affiliations:

[a] Graduate School of Sciences and Technology for Innovation, Yamaguchi University, Yoshida 1677-1, Yamaguchi 753-8515, Japan

[b] Faculty of Agriculture, Yamaguchi University, Yoshida 1677-1, Yamaguchi 753-8515, Japan

[c] Advanced Technology Institute, Yamaguchi University, Yoshida 1677-1, Yamaguchi 753-8515, Japan

[d] Kazusa DNA Research Institute, 2-6-7 Kazusa-kamatari, Kisarazu Chiba, 292-0818 Japan

[e] Science Research Center, Organization for Research Initiatives, Yamaguchi University, Yoshida 1677-1, Yamaguchi 753-8515, Japan

[f] The United Graduate School of Agricultural Science, Tottori University, Tottori 680-8553 Japan

***Corresponding author:** Jun'ichi Mano

E-mail: mano@yamaguchi-u.ac.jp

Present address: The Institute of Advanced Energy, Kyoto University, Gokasho, Uji, 611-0011 Japan

†**Present address:** Graduate School of Agriculture, Kobe University, Rokkodai-cho 1-1, Kobe, 657-8501 Japan

ABSTRACT

Reactive carbonyl species (RCS), such as acrolein (Acr), arise from lipid peroxide degradation and are highly cytotoxic. To identify natural RCS scavengers, extracts of 46 angiosperm species were prepared with 80% ethanol and evaluated for Acr-trapping activity using an HPLC-based assay. Strong activities were found in diverse families, including garlic, spinach, and avocado. In garlic, the active metabolite was identified as *S*-allyl-L-cysteine sulfoxide, characteristic of Allium species, which trapped up to two Acr molecules at its amino group. Its analog, *S*-(1*E*)-propenyl-L-cysteine sulfoxide (isoalliin), the major onion constituent, displayed even stronger activity, surpassing established scavengers such as carnosine and epigallocatechin gallate. These findings highlight *S*-alk(en)yl-L-cysteine sulfoxides as potent secondary antioxidants and suggest that additional, structurally diverse RCS-scavenging compounds remain to be discovered across the plant kingdom.

KEYWORDS: *acrolein*, *alliin*, *isoalliin*, *methiin*, *reactive carbonyl species*

48 Plant life is exposed to potential threats from reactive oxygen species (ROS). During
49 photosynthesis in plants, singlet oxygen ($^1O_2$) and superoxide radical (O_2^-) are constantly
50 produced in chloroplasts (Asada 2006). Furthermore, the H_2O_2 generation flux in
51 peroxisomes in illuminated leaves of C3 plants reaches 25% of the flux of CO_2 fixation on
52 electron base. This is approximately 50 times greater than the ROS generation flux associated
53 with mitochondrial respiration (Foyer and Noctor, 2003). When plants suffer environmental
54 stress, i.e. any changes in the surrounding environmental conditions that are not favorable for
55 a plant, ROS production in the cells are increased due to the disturbance of metabolism (for
56 example, the rate of CO_2 fixation in leaves decreases at low temperatures or under drought).
57 ROS oxidize biomolecules such as proteins, nucleic acids and lipids, thereby impairing their
58 functions and damaging cells. As a defense system against ROS, plant cells are richly
59 equipped with multiple types of ROS-scavenging enzymes and antioxidants, thereby keeping
60 ROS concentrations low enough.
61 ROS exert their biological functions also via the secondary products 'reactive carbonyl
62 species (RCS)'. RCS is a collective name of the α,β-unsaturated aldehydes and ketones such
63 as acrolein (Acr) and 4-hydroxy-(*E*)-2-nonenal (HNE) that are formed via the degradation of
64 lipid peroxides (Esterbauer et al. 1991, Aldini et al. 2005, Mano 2012). An RCS molecule
65 readily forms an adduct with a protein at the thiol-, amino-, or imidazole group via Michael
66 addition of its β-carbon (Esterbauer et al. 1991), and cause alterations of the protein function

67 (Wible and Sutter 2017). In plants, more than a dozen types of RCS occur (Schauenstein et
68 al. 1977, Mano 2012) and their levels are increased under oxidative stress conditions (Yin et
69 al. 2010, Yamauchi et al. 2012, Biswas and Mano 2015, Roach et al. 2018, Sultana et al.
70 2022, 2024). Rises of RCS levels have significant physiological impacts. For example, the
71 genetic enhancement of the RCS-scavenging enzyme 2-alkenal reductase (AER) (Mano et al.
72 2002, 2005) in transgenic plants suppressed the increases in RCS levels due to salt stress
73 (Sultana et al. 2024), aluminium stress (Yin et al. 2010) and light stress (Mano et al. 2010)
74 and thereby conferred stress tolerance. Vice versa, the genetic deficiency of aldehyde
75 alkenal/one reductase (Yamauchi et al. 2012) and aldehyde oxidase (Srivastava et al. 2017,
76 Nurbekova et al. 2021) made the plants more susceptible to oxidative stress or senescence.
77 The plant defense system against RCS toxicity consists of several types of enzymes and small
78 molecules, as the system against ROS. As for enzymatic defense, several classes of enzymes
79 with distinct RCS-detoxifying reactions have been characterized such as AER (Mano et al.
80 2002, 2005), glutathione transferase tau isozymes (Mano et al. 2017, 2019a,b) and aldehyde-
81 scavenging enzymes such as aldo-keto reductase (Yamauchi et al. 2011), aldehyde
82 dehydrogenase (Sunker et al. 2003) and aldehyde oxidase (Srivastava et al. 2017, Nurbekova
83 et al. 2021).
84 RCS-scavenging small molecules also occur in plants. Thiol compounds such as cysteine
85 (Cys) and the reduced form of glutathione are excellent RCS scavengers (Esterbauer et al.

86 1975). Various polyphenols also have the RCS scavenging ability. Zhu et al. (2009)
87 compared the RCS scavenging ability of a dozen tea polyphenols *in vitro* and found that nine
88 of them, including epigallocatechin gallate (EGCG), showed a high Acr-scavenging activity.
89 The reaction of EGCG and Acr starts with a nucleophilic attack of the carbon at position 8 on
90 the EGCG A-ring on the *β*-carbon of Acr, thus forming a Michael adduct. Subsequent aldol
91 condensation produces a ring structure (Huang, et al., 2020). One EGCG molecule can bind
92 up to three Acr molecules (Sugimoto, et al., 2021). Acr-scavenging reactions have been also
93 characterized for other polyphenols and their glycosides such as resveratrol, hesperetin
94 (Wang, et al., 2015), ferulic acid (Tao, et al., 2019), pelargonidin (Colzani, et al., 2018),
95 myricetin (Zhang, et al., 2020) and cyanidin-3-*O*-glucoside (Song, et al., 2021).
96 Amino compounds also have RCS-scavenging potential. The primary amino group in γ-
97 aminobutyric acid (GABA), L-Ala and L-Ser serves as a Michael acceptor to bind up to two
98 molecules of Acr (Jiang et al. 2020a, Zou et al. 2021). Recently it was reported that *S*-allyl
99 cysteine sulfoxide (alliin), an amino acid typical of *Allium* species, can scavenge Acr at a
100 high speed although the reaction mechanism has yet to be clarified (Uemura et al. 2023).
101 Theophylline, a purine derivative found in tea, forms a Michael adduct between its secondary
102 amine and the *β*-carbon of Acr at a high rate (Jiang, et al., 2020b). Interestingly, animals
103 contain RCS-scavenging dipeptides carnosine, homocarnosine, and anserine (Aldini et al.
104 2002) in brain and muscle. The amino and imidazole groups of these histidine-containing

105 dipeptides react as Michael acceptors (Aldini et al., 2005), allowing them to be excellent RCS
106 scavengers (Aldini et al., 2002; Liu et al., 2003; Carini et al., 2003). Exogenous application
107 of these dipeptides to plant cells or seedlings suppressed the RCS levels and mitigated
108 oxidative injury, without affecting ROS levels (Biswas and Mano, 2015; Sultana et al., 2022),
109 showing that RCS-scavenging compounds can protect plants as the "secondary antioxidants".
110 In this study, we aimed at discovering RCS-scavenging compounds in plants. Employing Acr
111 as a representative RCS, we evaluated RCS-scavenging ability of dozens of angiosperms.
112 Garlic cloves showed the highest content of Acr-scavenging ability, which was attributed to
113 alliin, a garlic-typical amino acid. We found that isoalliin and methiin, the cysteine
114 derivatives relative to alliin, also showed excellent Acr-scavenging ability and revealed the
115 reaction mechanism. Potential of plant specialized compounds as the secondary antioxidants
116 is discussed.
117

118 **Materials and Methods**

119 ***Chemicals*** Alliin and methiin were purchased from LKT Laboratories (Saint Paul, MN).
120 Carnosine, fluorescein, and HNE dimethyl acetal (HNE-DMA) were purchased from Sigma-
121 Aldrich Japan (Tokyo), and isoalliin from Nagara Science Co. (Gifu, Japan). Anserine nitrate
122 was purchased from Fujifilm Wako Pure Chemical (Osaka, Japan). 2,4-
123 Dinitrophenylhydrazine (DNPH), purchased from Fujifilm Wako, was purified by

124 recrystallization in acetonitrile and kept in acetonitrile until use (Mano et al. 2022). All other
125 chemicals were of analytical grade. Acr was prepared on the day of use by hydrolysis of the
126 acetal, as follows. Acrolein dimethyl acetal (Tokyo Chemical Industry, Tokyo, Japan) was
127 dissolved in 100 mM HCl aqueous solution at 40˚C for 40 min. The solution was then
128 neutralized with $NaHCO_3$ and further incubated at 25˚C for 2 h. The concentration of Acr was
129 determined from the absorbance at 215 nm with an extinction coefficient of 15.0 mM^{-1} cm^{-1}
130 (in water).

131 ***Plant Materials*** Bamboo (*Phyllostachys heterocycla*) shoots and yuzu (*Citrus junos*) fruits
132 were harvested from Yamaguchi University's experimental field. Following materials of fresh
133 plants were purchased from grocery stores in Yamaguchi (Japan) between April and December
134 2018: Apple (*Malus domestica*) fruits, asparagus (*Asparagus officinalis*) shoots, avocado
135 (*Persea americana*) fruits, bell pepper (*Capsicum annuum* 'Grossum') fruits, bitter melon
136 (*Momordica charantia* var. *pavel*) fruits, broccoli (*Brassica oleracea* var. italica) buds, carrot
137 (*Daucus carota* subsp. *sativus*) roots, cherry (*Cerasus avium*) fruits, chestnuts (*Castanea*
138 *crenata*), Chinese yam (*Dioscorea polystachya*) roots, common ginger (*Zingiber officinale*)
139 rhizomes, edible burdock (*Arctium lappa*) roots, eggplant (*Solanum melongena*) fruits, fig
140 (*Ficus carica*) fruits, garlic (*Allium sativum*) cloves, grape (*Vitis labruscana* 'Pione') fruits,
141 green onion (*Allium fistulosum*) leaves, guava (*Psidium guajava*) fruits, Haskap berry
142 (*Lonicera caerulea* var. *emphyllocalyx*) fruits, Indian gooseberry (*Phyllanthus emblica*) fruits,

143 Japanese apricot (*Prunus mume*) fruits, Japanese butterbur (*Petasites japonicus*) stalks,
144 Japanese ginger (*Zingiber mioga*) shoots, Jun-sai (*Bransenia shreberi*) leaves, Kaki persimmon
145 (*Diospyros kaki*) fruits, kiwifruit (*Actinidia deliciosa*) fruits, Korean lettuce (*Lactuca sativa*)
146 leaves, loquat (*Rhaphiolepis bibas*) fruits, lotus (*Nelumbo nucifera*) rhizomes, Mandarin
147 orange (*Citrus unshiu*) fruits, mulkhiya (*Corchorus olitorius*) leaves, okra (*Abelmoschus*
148 *esculentus*) fruits, onion (*Allium cepa*) bulbs, parsley (*Petroselinum crispum*) leaves, pea
149 (*Pisum sativum*) seeds, perilla (*Perilla frutescens* var. *crispa*) leaves, pitaya (*Hylocereus*
150 *undatus*) fruits, plum (*Prunus salicina*) fruits, spinach (*Spinacia oleacea*) leaves, star fruit
151 (*Averrhoa carambola*) fruits, strawberry (*Fragaria* × *ananassa*) achenes, taro (*Colocasia*
152 *esculentai*) tubers, watermelon (*Citrullus lanatus*) fruits, and white radish (*Raphanus*
153 *sativus* var. *hortensis*) roots.

154 ***Plant Extract Preparation*** An edible portion (10 g) taken from a fresh sample was
155 homogenized in 80% (v/v) ethanol (20 mL) using a kitchen blender and filtered through a layer
156 of Miracloth (Sigma-Aldrich Japan). The filtrate was acidified with HCl (10 mM final) to
157 facilitate protein precipitation. It was centrifuged after 10 minutes of incubation at 25˚C, and
158 the resulting supernatant was neutralized with sodium bicarbonate. The volume of
159 deproteinized extract was measured.

160 ***Determination of the Acr-scavenging ability*** A reaction mixture containing 200 μM Acr, 50
161 mM potassium phosphate pH 6.8, and a plant extract was incubated at 30˚C for 10 min. One

162 volume of the mixture was then added to 6.35 volumes of acetonitrile containing 4 mM DNPH

163 and 0.4 M formic acid and incubated at 30˚C for 60 min. The resulting hydrazone solution was

164 filtered through a 0.45 μm filter (Millex LH; Merck, Darmstadt, Germany) and analyzed by

165 HPLC, as follows. The hydrazone solution (10 μL) was injected into a Zorbax ODS column

166 (4.6 × 250 mm, 5 μm; Agilent Technologies Japan, Hachioji, Japan) kept at 40˚C and separated

167 in a 1.0 mL min^{-1} flow of 75% (v/v) acetonitrile in water (isocratic elution) with a high-pressure

168 pump (2690 Separation Module, Waters Corp., Milford, MA). The hydrazone was detected

169 with a UV-visible detector (2487 Absorbance Detector, Waters) at 370 nm. This concentration

170 was chosen based on reported values in Arabidopsis seedlings under salt stress (Sultana et al.

171 2022), corresponding to ~200 μM tissue concentrations, thereby approximating

172 physiologically relevant stress levels.

173 The decrease rate (v) of Acr concentration in the reaction mixture (in mol Acr consumed s^{-1} L^{-}

174 ^{1}) was used to calculate the Acr-scavenging ability of the plant extract per unit volume (in mol

175 Acr s^{-1} (L extract)$^{-1}$) by multiplying v by the volume ratio P (reaction mixture/plant extract) as

176 follows:

177 Acr-scavenging ability per unit volume of plant extract (mol s^{-1} (L extract)$^{-1}$)

178 $= v$ (mol Acr scavenged L^{-1} s^{-1}) $\times P$

179 The Acr-scavenging ability content in the original sample, as mol Acr consumed s^{-1} (g

180 sample)$^{-1}$, was then calculated from the extraction efficiency E (L extract (g sample)$^{-1}$) as

181 follows:

182 Acr-scavenging ability content (mol s^{-1} (g sample)$^{-1}$)

183 = Acr-scavenging ability of the extract (mol s^{-1} L^{-1}) × 1 (L) × E (L extract (g sample)$^{-1}$)

184 ***Purification of the Acr-scavenging component from garlic cloves*** Garlic cloves (40 g) were

185 homogenized in 80% (v/v) ethanol (80 mL) using a kitchen blender, filtered through two layers

186 of Miracloth, and centrifuged to remove insoluble debris. The supernatant was freeze-dried to

187 obtain 7.6 g of material, which was dissolved in distilled water (15 mL) and loaded onto a

188 preparative hydrophilic column (Universal Column Premium Amino 30 μm, 3.0 × 16.5 cm;

189 Yamazen Corp., Osaka, Japan) with a medium pressure chromatography system (EPCLC AI-

190 580; Yamazen Corp.) equipped with a detector (fixed wavelength at 254 nm). Chromatography

191 was performed at a flow rate of 20 mL/min under the following solvent conditions: solvent A:

192 acetonitrile:10 mM ammonium acetate in water (88:12, v/v); solvent B: acetonitrile:100 mM

193 ammonium acetate in water (1:1, v/v). The gradient program consisted of 0–16 min isocratic

194 elution of 0% B, 16–56 min of a linear gradient from 0% to 100% B, and 56–80 min isocratic

195 elution of 100% B. The fraction size was 20 mL. Each fraction was freeze-dried and then

196 dissolved in 2 mL of distilled water, and its Acr-scavenging ability was determined as

197 described above. The most active fraction was then separated on a Unison UK-Amino Column

198 (3 μm, 4.6×100 mm; Imtakt, Kyoto, Japan) with an HPLC apparatus equipped with an LH-40
199 liquid handler and an SPD-10AVP UV-VIS detector (Shimadzu Corp., Kyoto, Japan).
200 Chromatography was performed at a flow rate of 0.6 mL min^{-1} with the following multistep
201 gradient elution: 0–10 min isocratic elution of 0% B; 10–35 min of a linear gradient from 0%
202 to 100% B; 35–50 min isocratic elution of 100% B; 50–55 min of a linear gradient from 100%
203 to 0% B; and, finally, 55–90 min isocratic elution of 0% B. The fraction size was 1.8 mL. The
204 elution profile was monitored at 220 nm for nonspecific detection of organic substances. After
205 40 separation runs (50 μL injection per run), identical fractions were accumulated, freeze-dried,
206 and dissolved in a smaller volume to determine the Acr-scavenging ability.
207 ***LC-MS/MS analysis*** Chromatographic separation was performed on a hydrophilic Intrada
208 Amino Acid column (3 μm, 3 × 100 mm; Imtakt) with a Vanquish UHPLC System (Thermo
209 Fisher Scientific, Waltham, MA). A 5-μL aliquot of the sample was injected into the column
210 and eluted at a flow rate of 0.4 mL min^{-1} under the following solvent conditions: solvent A:
211 0.3% (v/v) in acetonitrile; solvent B: 0.1 M ammonium formate in water:acetonitrile (80:20,
212 v/v). The gradient program was as follows: 0–10 min isocratic elution of 15% B; 10–25 min
213 of a linear gradient from 15% to 60% B; 25–40 min isocratic elution of 60% B; 40–45 min of
214 a linear gradient from 60% to 15% B; and finally 45–50 min isocratic elution of 15% B. The
215 column temperature was set to 40˚C. Mass spectra were acquired using an Orbitrap Exploris
216 120 mass spectrometer (Thermo Fisher Scientific) equipped with an H-ESI source, with

217 acquisition in positive ion mode. The source parameters were as follows: capillary voltage of
218 3.5 kV in positive ion mode, ion transfer tube temperature of 325˚C, vaporizer temperature of
219 350˚C, sheath gas flow of 50 units, auxiliary gas flow of 10 units, and sweep gas of 1 unit. A
220 full scan was performed in the mass-to-charge ratio (*m*/*z*) range of 100–1000, with a resolution
221 of 120,000 at *m*/*z* 200. Tandem MS information was acquired in tMS^2 mode with a resolution
222 of 12,000 and HCD collision energies of 15, 30, and 45.
223

224 **Results and Discussion**

225 ***Comparison of Acr-scavenging ability of plants***

226 For choosing a starting material suitable for purifying RCS-scavenging compounds, we first
227 collected various plant samples across diverse angiosperm lineages. To obtain samples in such
228 a variety in short time, we obtained them (46 species in total), mainly fruits and vegetables,
229 from local retail stores (see Materials and Methods). Because polyphenols have been
230 extensively investigated as acrolein scavengers (Colzani, et al., 2018; Huang, et al., 2020;
231 Sugimoto, et al., 2021; Tao, et al., 2019; Wang, et al., 2015; Zhang, et al., 2020; Zhu, et al.,
232 2009), we aimed at polar compounds in this study. We chose 80% ethanol as an extraction
233 medium, which is preferable to extracting more polar compounds than polyphenols (Phahom
234 and Mano, 2022). This extract was deproteinized by acid treatment, then neutralized, and its
235 Acr-scavenging rate was determined. To survey RCS scavengers that can react rapidly with

236 Acr, we determined Acr consumption in the initial 10 minutes in our assay. The initial Acr
237 concentration was set at 200 μM, mimicking physiological concentration, which was estimated
238 on the following observation. A typical Acr content in salt-stressed *A. thaliana* seedlings is 200
239 nmol (g fresh weight)$^{-1}$ (Sultana, et al., 2022). From this value, Acr concentration of 200 μM
240 in the tissue was calculated on a simple assumption that the Acr molecules occur in the tissue
241 in a homogenous solution of 1 mL volume per gram tissue weight. The reaction temperature
242 was set at 30˚C to simulate field conditions.

243 Fig. 1 summarizes the Acr-scavenging ability on the fresh weight base of the plant materials.
244 Most plant materials showed significant levels of Acr-scavenging ability, thus indicating that
245 many plants contain Acr-scavenging compounds. The highest Acr-scavenging ability content
246 (in nmol Acr scavenged s^{-1} (g fresh weight)$^{-1}$) were 1.39 for garlic cloves, 0.99 for spinach
247 leaves, 0.96 for avocado fruits, 0.92 for lotus rhizomes, 0.91 for broccoli buds, 0.82 for
248 chestnuts, 0.70 for bamboo shoots, 0.67 for onion bulbs, and 0.65 for both Chinese yam roots
249 and white radish roots. These plants, when placed in the angiosperm phylogeny tree (Cole, et
250 al., 2019), were distributed to different orders of taxa (Fig. 1). We chose garlic cloves as the
251 starting material for purification to identify an Acr-scavenging compound.

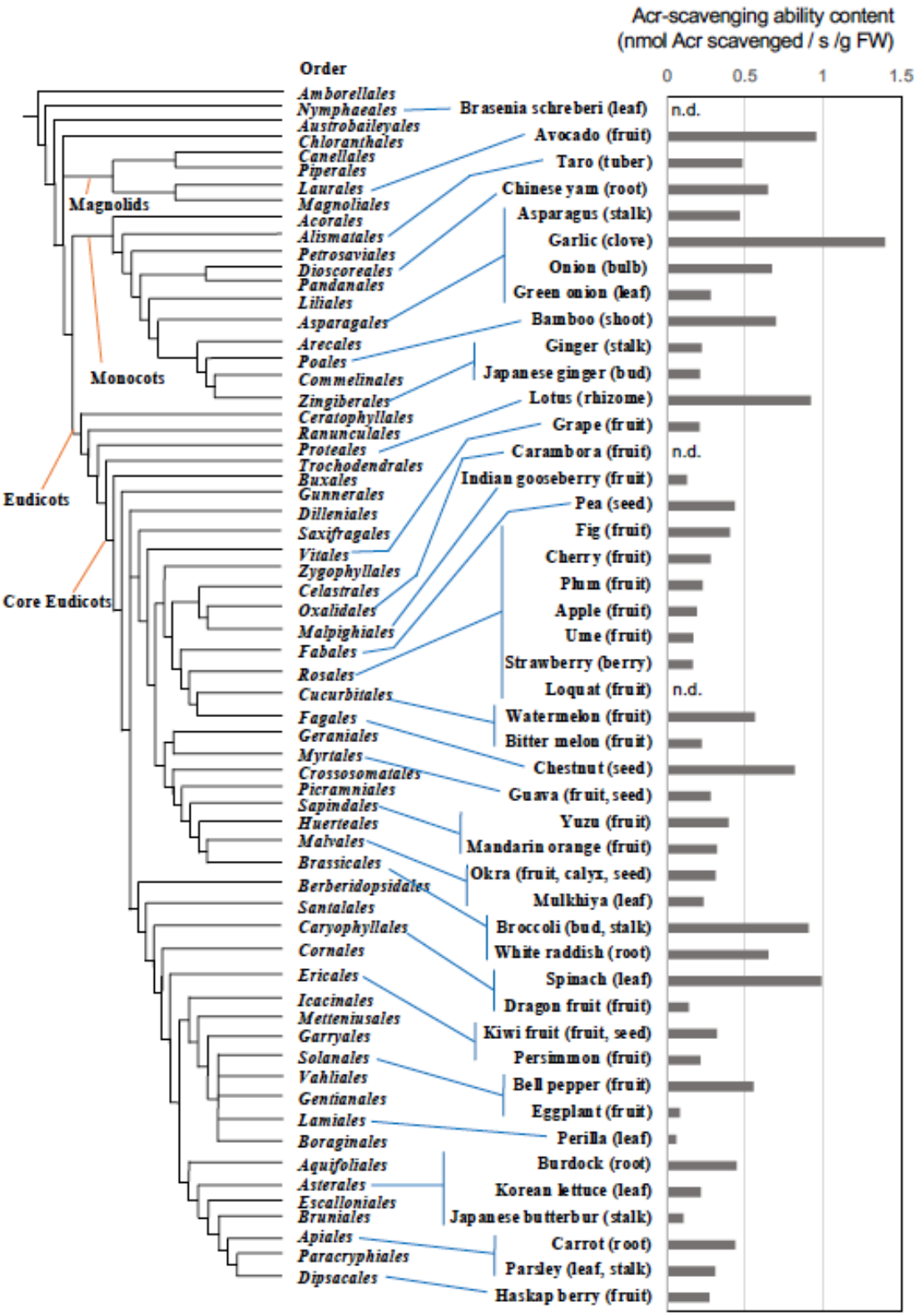

Figure 1. Acr-scavenging ability contents of plant materials. Plant extracts (80% ethanol) were deproteinized, neutralized, and tested for the Acr-scavenging ability as in Materials and Methods. Average of two runs. The phylogenic tree was constructed using the Angiosperm Phylogeny Poster (Cole et al. 2019) as a guide.

252

253

254 ***Purification of Acr-scavenging components from garlic extract***

255 Garlic clove extract was first separated by preparative amino column chromatography
256 (Supplementary Fig. S1A), which showed a single prominent peak of Acr-scavenging ability
257 in fractions #13, #14, and #15. We scaled up the sample amount and the column size, as
258 described in the Materials and Methods section, collected the active fractions, concentrated and
259 purified them using an analytical HPLC column. The resulting fraction #8 had a high Acr-
260 scavenging ability (Supplemental Fig. S1B). We then analyzed this fraction by LC-MS/MS.
261 Total ion chromatography (*m*/*z* 100–1000) revealed two major components: a broad peak
262 eluted at 15.3–16.6 min with *m*/*z* 178.0528 and a narrow peak at 18.87 min with *m*/*z* 258.1096
263 (Fig. 2A, black trace).

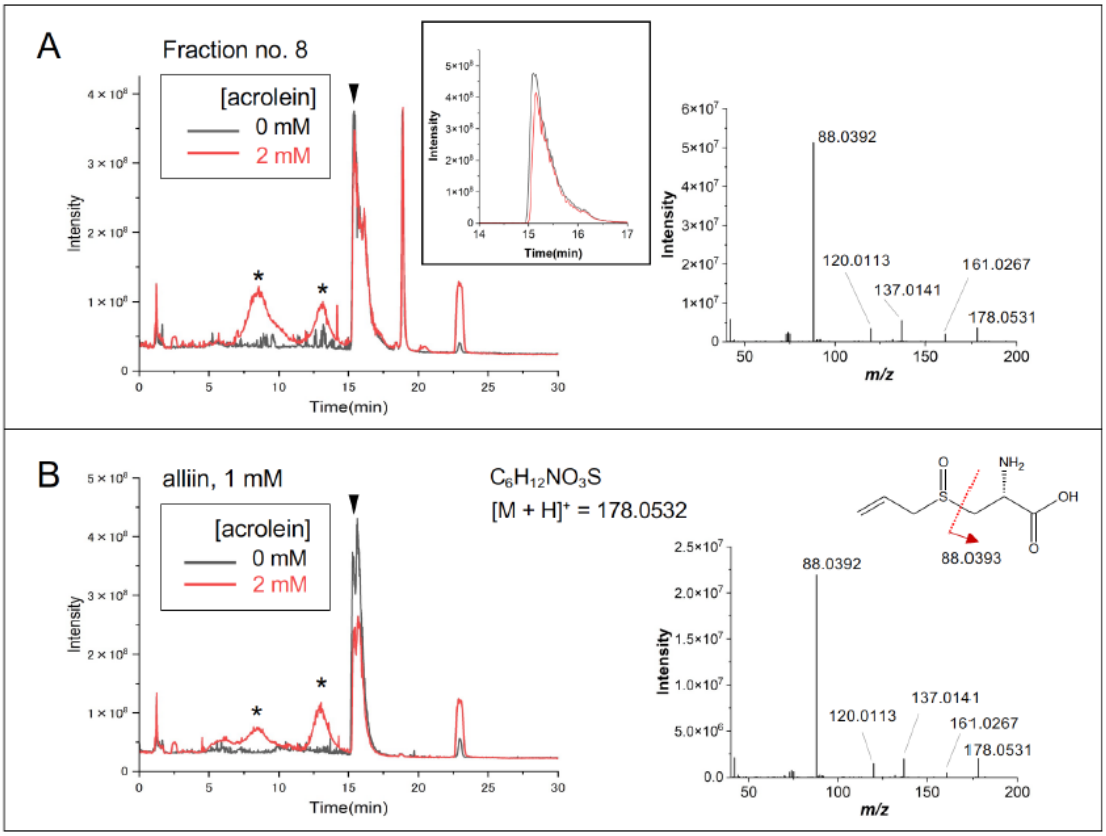

Figure 2. LC-MS/MS evidence that alliin is the acrolein-scavenging substance in the fraction no. 8 from the Unizon UK-Amino Column.

To clarify which component is the Acr scavenger, we mixed fraction #8 with Acr and examined the changes in the total ion chromatogram. The addition of Acr at 2 mM resulted in a significant decrease in the 15.3–16.6 min peak (Fig. 2A, inset), while that of the 18.87 min peak was unchanged, thus suggesting that the *m/z* 178.0528 signal represented the Acr scavenger in fraction #8. Addition of Acr to fraction #8 generated two new broad peaks at 8.57 (*m/z* 290.1056) and 13.16 min (*m/z* 234.0795) (Fig. 2A, asterisks). The *m/z* values of these peaks matched hypothetical Acr adducts to the *m/z* 178.0528 compound; the 13.16 min peak

271 corresponded to a mono-Acr adduct (mass increment 56.0265, matching the molecular weight

272 of Acr (C_3H_4O)), and the 8.57 min peak a di-Acr adduct (mass increment 112.0526).

273 Assuming that the *m*/*z* 178.0528 ion represents a $[M + H]^+$ ion, the elemental composition

274 of the molecule was deduced as $C_6H_{11}NO_3S$. Retrieval of the corresponding compounds in

275 the databases AraCyc (Mueller, et al., 2003), PlantCyc (Plant Metabolic Network (PMN):

276 https://pmn.plantcyc.org/organism-summary?object=PLANT, on www.plantcyc.org, Jan 15,

277 2022), and KEGG (Kanehisa, et al., 2000) using the software package Compound Discoverer

278 3.0 (Thermo Fisher Scientific), resulted in *S*-allyl-cysteine sulfoxide (alliin; $C_6H_{11}NO_3S$,

279 177.22 g mol^{-1}) as the most probable candidate.

280 Alliin is an amino acid sulfoxide characteristic of garlic, accounting for about 30% (w/w) of

281 total free amino acids in garlic cloves (Ueda, et al., 1991), and is a precursor of allicin, the

282 major compound of garlic odor (Stoll and Seebeck, 1948). In the LC-MS/MS analysis,

283 authentic L-alliin eluted as a broad peak ranging from 15.2–16.7 min with an *m*/*z* of 178.0532

284 (Fig. 2B). The MS^2 spectrum of this parent ion (*m*/*z* 178.0532) matched the spectrum of the

285 *m*/*z* 178.0528 ion of the Acr scavenger in fraction #8 (Fig. 2A). The addition of Acr to alliin

286 decreased the alliin peak and generated two broad peaks at 8.20 (*m*/*z* 290.1056) and 13.02 min

287 (*m*/*z* 234.0795) (Fig. 2B), as observed for fraction #8. Thus, the Acr-scavenging component in

288 the purified fraction was identified as alliin.

Reaction mechanism of alliin with Acr Uemura et al. (2023) has reported that alliin has a high capacity to scavenge Acr. Its reaction mechanism with Acr, yet to be elucidated, could be similar to that of an amino compound; i.e. the Michael addition of the β-carbon to the amino nitrogen, and the second addition of Acr to the same nitrogen, followed by the intramolecular aldol condensation to form a nitrogen-containing heterocycle (Carini et al. 2003). When alliin was incubated with Acr, larger MS signals of the mono-Acr adduct (*m/z* 234.0795, eluted at 8.20 min) and the di-Acr adduct (*m/z* 290.1056, 13.02 min) were observed as increasing concentration of Acr (Fig. 3A, B). In addition, another signal at *m/z* 272.0950 arose in higher Acr concentration (Fig. 3C). On the assumption that it represented a $[M + H]^+$ ion, the atomic composition of the compound was deduced as $C_{12}H_{17}NO_4S$. We presumed that this signal corresponded to a dehydrated product of the di-Acr adduct.

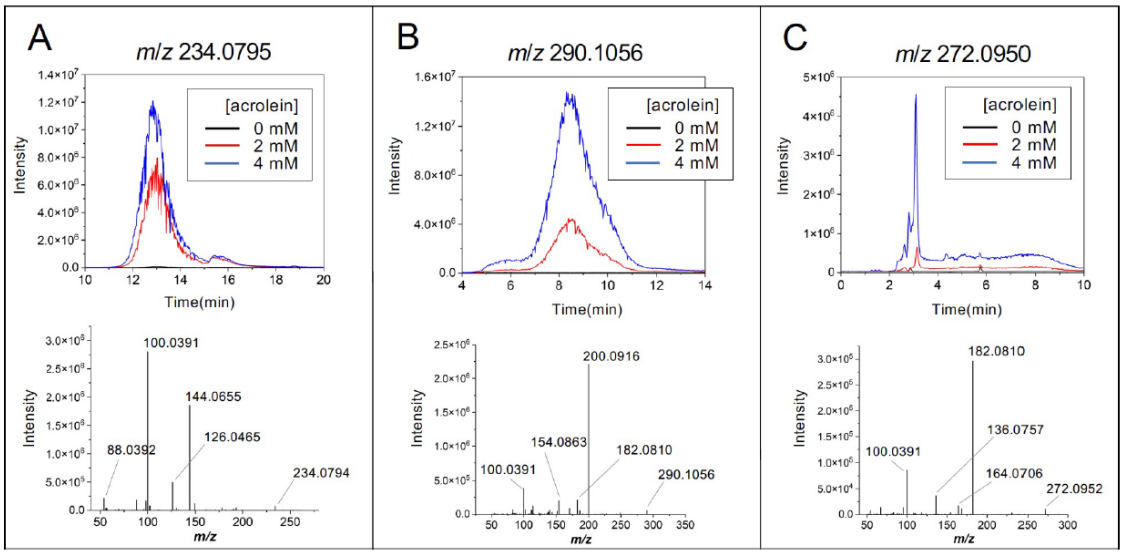

Figure 3. LC-MS/MS results of alliin-acrolein adducts.

301 We have purified this putative dehydrated product of the di-Acr adduct and determined its
302 structure with NMR. The deduced structure corresponded to the N^b-(3-formyl-3,4-
303 dehydropiperidino) derivative of alliin (Table 1), indicating that the amino group of alliin
304 accepted two molecules of Acr, as expected. Specifically, one Acr molecule adds to the amino
305 group (Michael-type reaction), then the resulting secondary amino group undergoes Michael
306 addition with another Acr molecule to form the $(Acr)_2$ adduct, which then undergoes aldol
307 condensation to form a nitrogen-containing heterocycle (Figure 4). The MS^2 spectra for the
308 Acr adducts support this mechanism; the spectrum for the mono-Acr adduct contained a
309 product ion at *m/z* 144.0655, the deduced atomic composition for which ($C_6H_{10}NO_3$) matched
310 the fragment generated by cleavage between the sulfur atom and the *β*-carbon of the amino
311 acid, the same cleavage position as in alliin (Fig. 2B). Similarly, the MS^2 spectra of the di-Acr

Table 1. ^{1}H NMR (400 MHz) and ^{13}C NMR (500 MHz) chemical shift data of the purified adduct of *m/z* 272.0950. Deduced structure of the dehydrated product of $(Acr)_2$-alliin adduct and a possible LC-MS/MS fragment ion structure are shown.

NMR data			Structural formula of the dehydrated product of $(Acr)_2$-alliin adduct	Fragment ion (+) of LC-MS/MS
No.	δ_H	δ_C		
1	5.52	124.85	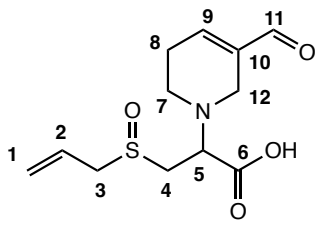	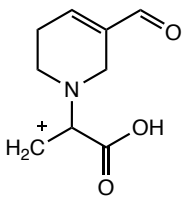
2	5.94	125.03		
3	3.60, 3.80	54.2		
4	3.27, 3.33	49.97		
5	3.7	63.68		
6	-	174.82		
7	2.87, 3.06	45.9		
8	2.61	26.81		
9	7.18	152.41	**exact mass 271.08728**	***m/z* 182.0810**
10	-	138.06		
11	9.35	195.6		
12	3.5	45.48		

312 adduct and its dehydrated product contained product ions at *m/z* 200.0917 (Fig. 3B) and *m/z*

313 182.0811 (Fig. 3C), which correspond to the fragments at the same cleavage position of the

314 deduced compounds, respectively. This formation parallels mechanisms described for

315 histidine-containing dipeptides (Carini et al. 2003), where successive Michael additions are

316 followed by intramolecular condensation (Figure 4).

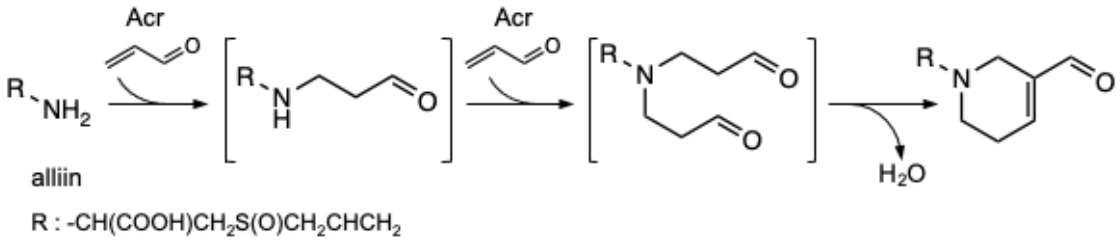

Figure 4. Possible reactions of alliin (R-NH_2) with Acr.

317

318

319 ***Comparison of the Acr-scavenging ability of S-alk(en)yl cysteine sulfoxides, amino***

320 ***compounds, and polyphenols*** Plants in the *Allium* family are rich in alliin-analogous *S*-

321 alk(en)yl cysteine sulfoxides, such as *S*-propenylcysteine sulfoxide (isoalliin) in onion (*A.*

322 *cepa*) and *S*-methylcysteine sulfoxide (methiin) in Oriental garlic (*A. tuberosum*) (Yamazaki,

323 et al., 2011). Isoalliin and methiin also formed mono-Acr and $(Acr)_2$ adducts and the

324 dehydration product of the $(Acr)_2$ adduct, as did alliin (Supplementary Fig. S3 and S4). The

325 Acr-scavenging rates of these *S*-alk(en)yl cysteine sulfoxides were 120–150 μM Acr in 30 min,

326 when the reaction was started with 1 mM Acr and 1 mM scavenger (Table 2A). These rates

327 were comparable to, or even higher than, those for carnosine and anserine, Acr-scavenging
328 dipeptides in animals (Carini, et al., 2003; Spaas, et al., 2021).
329 As compared with broader variety of amino compounds, these *S*-alk(en)yl cysteine sulfoxides
330 excelled GABA and most of protein-constituting amino acids such as Met, His, Lys, Arg and
331 Gly for the Acr-scavenging rate. Such high Acr-scavenging rate for *S*-alk(en)yl cysteine
332 sulfoxides appears to be attributed to the presence of sulfoxide close to the amino carbon.
333 Indeed, methionine sulfoxide, in which the sulfoxide is one carbon further away, showed a
334 significantly faster Acr-scavenging rate than other amino acids lacking a sulfoxide although its
335 rate was slower than *S*-alk(en)yl cysteine sulfoxides (Table 2A).
336 We also compared the *S*-alk(en)yl cysteine sulfoxides with polyphenols that can scavenge
337 Acr. Isoalliin, methiin and alliin outperformed EGCG in scavenging Acr (Table 2A). We note
338 that assays of polyphenols (resveratrol, hesperetin) were conducted in 10% DMSO with longer
339 incubation times due to low solubility and slower reaction kinetics (Wang, et al., 2015).
340 Therefore, direct quantitative comparisons with amino acid sulfoxides should be made
341 cautiously. To compare alliin with resveratrol and hesperetin, a separate experiment was
342 performed in 10% DMSO solution and reaction time was set to 5 h (Table 2B). Under these
343 conditions, alliin scavenged Acr faster than EGCG, resveratrol, and hesperetin. Theophylline,
344 another type of Acr scavenger (Jiang, et al., 2020b) showed an Acr-scavenging rate comparable
345 to that for hesperetin and much slower than that for EGCG and alliin (Table 2B).

346

347 **Table 2** (A) Comparison of Acr-scavenging rate of amino compounds. Acr (1 mM) was
348 incubated with a scavenger (1 mM) in 50 mM potassium phosphate, pH 7.0, at 30˚C for 30
349 min. The remaining Acr was determined by HPLC after derivatization with DNPH, as
350 described in the Materials and Methods section. Acr consumption (concentration in the
351 reaction mixture) in 30 min is shown. (B) Comparison of Acr-scavenging rate for alliin,
352 polyphenols, and theophylline. Acr (1 mM) was incubated with a scavenger (1 mM) in 10%
353 DMSO, 50 mM potassium phosphate, pH 7.0, at 30˚C for 5 h. Acr consumption in 5 h is
354 shown. The values shown are the average and standard error of three independent runs.
355 Different letters in the Statistics column represent significantly different values ($P < 0.05$,
356 Tukey's test).

A	Compound	Acr consumption (μM in 30 min)	Statistics
	Isoalliin	153.8 ± 6.5	a
	Methiin	144.5 ± 14.0	ab
	Alliin	126.8 ± 5.4	bc
	Carnosine	114.3 ± 1.3	cd
	Anserine	99.4 ± 5.5	de
	Methionine sulfoxide	86.0 ± 8.3	e
	Histidine	63.9 ± 6.0	f
	Lysine	59.5 ± 8.9	f
	Phenylalanine	57.5 ± 0.9	f
	EGCG	45.4 ± 5.2	f
	Arginine	44.7 ± 6.3	f
	Histamine	40.1 ± 8.4	fg
	Methionine	22.7 ± 8.7	gh
	GABA	10.6 ± 5.9	h
	β-Alanine	6.5 ± 3.7	h

357

B	Compound	Acr consumption (μM in 5 h)	Statistics
	Alliin	419.1 ± 3.0	a
	EGCG	282.0 ± 4.6	b
	Resveratrol	31.8 ± 1.5	c
	Hesperetin	18.9 ± 1.0	d
	Theophylline	17.9 ± 3.6	d

358

359 ***RCS scavenging compounds are present in many plant species*** Because RCS are secondary
360 toxic products derived from ROS, plants have evolved multiple enzymatic and non-enzymatic
361 mechanisms to mitigate their harmful effects (Mano et al. 2019a,b). In this study, we
362 established a method to evaluate the RCS-scavenging ability of plant extracts and demonstrated
363 that *S*-alk(en)yl cysteine sulfoxides, amino acids characteristic of *Allium* family, are highly
364 efficient Acr scavengers. Among them, isoalliin, the major sulfoxide in onion, exhibited the
365 strongest Acr-scavenging activity, surpassing not only its structural analog alliin but also other
366 well-known plant-derived and animal-derived scavengers. This finding identifies isoalliin as a
367 representative plant RCS scavenger and underscores the contribution of *Allium* metabolites to
368 the chemical defense system against carbonyl stress. Isoalliin concentrations in onion bulbs are
369 reported at 5–20 μmol g^{-1} FW (Yamazaki et al. 2011; Ueda et al. 1991). At these levels,
370 isoalliin would be comparable to stress-induced Acr accumulation, supporting its role as an in
371 planta scavenger.

372 It is noteworthy that the presence of a sulfoxide group in close proximity to the amino
373 carbon markedly enhances the Michael acceptor reactivity of the amino group, thereby
374 conferring the high RCS-scavenging capacity observed in S-alk(en)yl cysteine sulfoxides.
375 Consequently, the RCS-scavenging property of a compound appears to be governed by the
376 cooperative action of two or more functional groups, rather than by the reactivity of a single

377 moiety alone. More broadly, our findings suggest that structurally diverse, and as yet
378 unexplored, plant metabolites may play critical roles in mitigating oxidative damage through
379 RCS detoxification.
380
381
382 **ABBREVIATIONS**
383 Acr, acrolein; DNP-, dinitrophenylhydrazo-; DNPH, 2,4-dinitrophenylhydrazine; FW, fresh
384 weight; GSH, the reduced form of glutathione; HNE, 4-hydroxy-(*E*)-2-nonenal; LOOH, lipid
385 peroxide; RCS, reactive carbonyl species; ROS, reactive oxygen species.
386
387 **AUTHOR CONTRIBUTION**
388 Conceptualization: J. M. and D.S.; Investigation: A.H., N.T.; Methodology: J.M., C.N., A.H.,
389 N.T., Y.M., K.M.; Roles/Writing - original draft: A.H., N.T., Writing - review & editing; A.H.,
390 J.M., Funding acquisition: J.M., D.S.; Supervision: J.M.
391
392
393 **FIGURE LEGENDS**

394 **Fig 1.** Acr-scavenging ability contents of plant materials. Plant extracts (80% ethanol) were
395 deproteinized, neutralized, and tested for the Acr-scavenging ability as in Materials and

396 Methods. Average of two runs. The phylogenic tree was constructed using the Angiosperm

397 Phylogeny Poster (Cole et al. 2019) as a guide.

398 **Fig. 2.** LC-MS/MS evidence that alliin is the Acr-scavenging substance in fraction #8 using a

399 Unizon UK-Amino Column. A: Total ion chromatograms (*m*/*z* range 100–1000) of fraction

400 #8 with 2 mM Acr (red trace) and without it (black). The MS/MS spectrum of the *m*/*z*

401 178.0528 signal at 15.4 min is shown on the right. Inset: expanded chromatogram of the 15.1

402 min peak. B: Total ion chromatograms (*m*/*z* range 100–1000) of 1 mM alliin with 2 mM Acr

403 (red trace) and without it (black). The MS/MS spectrum of the *m*/*z* 178.0532 signal at 15.4

404 min (arrowhead) is shown on the right. Asterisks show possible Acr reaction products with

405 the scavenging compound (A) or with alliin (B).

406 **Fig. 3.** LC-MS/MS results for alliin-Acr adducts. An authentic alliin preparation (5 mM) was

407 mixed with various concentrations of Acr, incubated for 1 h, and subjected to LC-MS/MS

408 analysis. A: Extracted ion chromatograms of the mono-Acr adduct of alliin (*m*/*z* 234.0795). B:

409 Extracted ion chromatograms of the $(Acr)_2$ adduct (*m*/*z* 290.1056). C: Extracted ion

410 chromatograms of the dehydrated products from the di-Acr adduct (*m*/*z* 272.0950). The

411 corresponding parent ion MS/MS spectrum is shown at the bottom of panels A–C. This

412 formation parallels mechanisms described for histidine-containing dipeptides (Carini et al.

413 2003), where successive Michael additions are followed by intramolecular condensation.

414 Figure 4 illustrates this comparison explicitly.

415 **Fig. 4.** Possible reactions of alliin with Acr.

416

417 **ASSOCIATED CONTENTS**

418 Supporting information is available.

419 Two chromatographic results for the purification of Acr-scavenging substances from garlic

420 extract (Fig. S1), MS spectrum of the 15.42 min peak of fraction #8 (Fig. S2), LC-MS/MS

421 results for the reaction products of isoalliin and Acr (Fig. S3), and LC-MS/MS results for the

422 reaction products of methiin and Acr (Fig. S4).

423

424

425 **REFERENCES**

426 Aldini, G., Carini, M., Beretta, G., Bradamante, S., and Facino, R. M. (2002) Carnosine is a
427 quencher of 4-hydroxy-nonenal: through what mechanism of reaction? Biochem.
428 Biophys. Res. Commun. 298: 699-706.

429 Aldini, G., Facino, I., Beretta, G. and Carini, M. (2005) Carnosine and related dipeptides as
430 quenchers of reactive carbonyl speices: From structural studies to therapeutic
431 perspecitves. BioFactors 24: 77-87.

432 Aldini, G., Dalle-Donne, I., Facino, R. M., Milzani, A. and Carini, M. (2007) Intervention
433 strategies to inhibit protein carbonylation by lipoxidation-derived reactive carbonyls.
434 Med. Res. Rev. 27: 817-868, https://doi.org/10.1002/med.20073.

435 Aldini, G., Orioli, M., Rossoni, R., Savi, F., Braidotti, P., Vistoli, G., Yeum, K.-J., Negrisoli,
436 G. and Carini, M. (2011) The carbonyl scavenger carnosine ameliorates dyslipidaemia
437 and renal function in Zucker obese rats. J. Cell. Mol. Med. 15: 1339-1354.

438 Asada, K. (2006) Production and scavenging of reactive oxygen species in chloroplasts and
439 their functions. Plant Physiol. 141: 391-396.

440 Biswas, M. S. and Mano, J. (2015) Lipid peroxide-derived short-chain carbonyls mediate
441 hydrogen peroxide-induced and salt-induced programmed cell death in plants. Plant
442 Physiol. 168: 885–898.

443 Carini, M., Aldini, G., Beretta, G., Arlandini, E. and Facino, R. M. (2003) Acrolein-
444 sequestering ability of endogenous dipeptides: characterization of carnosine and
445 homocarnosine/acrolein adducts by electrospray ionization tandem mass
446 spectrometry. J. Mass Spectr. 38: 996-1006.

447 Cole, T. C., Hilger, H. H. and Stevens, P. (2019) Angiosperm Phylogeny Poster (APP) –
448 Flowering plant systematics. PeerJ Preprints 7: e2320v6

449 Colzani, M., Regazzoni, L., Criscuolo, A., Baron, G., Carini, M., Vistoli, G., Lee, Y.-M., Han,
450 S. I., Aldini, G. and Yeum, K.-J. (2018) Isotopic labelling for the characterisation of
451 HNE-sequestering agents in plant-based extracts and its application for the
452 identification of anthocyanidins in black rice with giant embryo. Free Rad. Res. 52:
453 896-906.

454 Esterbauer, H., Zollner, H. and Scholtz, N. (1975) Reaction of glutathione with conjugated
455 carbonyls. Z. Naturforsch. 30c 466-473.

456 Esterbauer, H., Schaur, R. and Zollner, J. H. (1991) Chemistry and biochemistry of 4-
457 hydroxynonenal, malonaldehyde and related aldehydes. Free Rad. Biol. Med. 11: 81-
458 128.

459 Foyer, C. H. and Noctor, G. (2003) Redox sensing and signalling associated with reactive
460 oxygen in chloroplasts, peroxisomes and mitochondria. Physiol. Plant. 119 355-364.

461 Huang, Q., Zhu, Y., Lv, L. and Sang, S. (2020) Translating in vitro acrolein-trapping capacities
462 of tea polyphenol and soy genistein to in vivo situations is mediated by the
463 bioavailability and biotransformation of individual polyphenols. Mol. Nutr. Food Res.
464 64: 1900274.

465 Jiang, K., Yin, Z., Zhou, P., Guo, H., Huang, C., Zhang, G., Hu, W., Ou, S. and Ou, J. (2020a)
466 The scavenging capacity of γ-aminobutyric acid for acrolein and the cytooxicity of the
467 formed adduct. Food Funct. 11: 7736.

468 Jiang, X., Zhang, D., Lu, Y. and Lv, L. (2020b) Acrolein-trapping mechanism of theophylline
469 in green tea, coffee, and cocoa: Speedy and successful. J. Agric. Food Chem. 68: 9718-
470 9724.

471 Kanehisa, M. and Goto, S. (2000) KEGG: Kyoto Encyclopedia of Genes and Genomes.
472 Nucleic Acids Res. 28: 27-30.

473 Knieper, M., Viehhauser, A. and Dietz, K.-J. (2023) Oxylipins and reactive carbonyls as
474 regulators of the plant redox and reactive oxygen species network under stress.
475 Antioxidants 12: 814.

476 Liu, Y., Xu, G. and Sayre, L. M. (2003) Carnosine 1nhibits (*E*)-4-hydroxy-2-nonenal-induced
477 protein cross-linking: structural characterization of carnosine−HNE adducts. Chem.
478 Res. Toxicol. 16: 1589-1597.

479 Mano, J. (2012) Reactive carbonyl species: their production from lipid peroxides, action in
480 environmental stress, and the detoxification mechanism. Plant Physiol. Biochem. 59:
481 90-97.

482 Mano, J., Torii, Y., Hayashi, S.-I., Takimoto, K., Matsui, K., Nakamura, K., Inzé, D.,
483 Babiychuk, E., Kushnir, S. and Asada, K. (2002) The NADPH:quinone
484 oxidoreductase P1-ζ-crystallin in Arabidopsis catalyzes the α,β-hydrogenation of 2-
485 alkenals: detoxication of the lipid peroxide-derived reactive aldehydes. Plant Cell
486 Physiol. 43:1445-1455.

487 Mano, J., Belles-Boix, E., Babiychuk, E., Inzé, D., Torii, Y., Hiraoka, E., Takimoto, K.,
488 Slooten, L., Asada, K. and Kushnir, S. (2005) Protection against photooxidative injury
489 of tobacco leaves by 2-alkenal reductase. Detoxication of lipid peroxide-derived
490 reactive carbonyls. Plant Physiol. 139: 1773–1783.

491 Mano, J., Tokushige, K., Mizoguchi, H., Fujii, H. and Khorobrykh, S. (2010) Accumulation
492 of lipid peroxide-derived, toxic α,β-unsaturated aldehydes (E)-2-pentenal, acrolein
493 and (E)-2-hexenal in leaves under photoinhibitory illumination. Plant Biotechnol. 27:
494 193–197.

495 Mano, J., Ishibashi, A., Muneuchi, H., Morita, C., Sakai, H., Biswas, M. S., Koeduka, T. and
496 Kitajima, S. (2017) Acrolein-detoxifying isozymes of glutathione transferase in
497 plants. Planta 245: 255-264.

498 Mano, J., Kanameda, S., Kuramitsu, R., Matsuura, N. and Yamauchi, Y. (2019)
499 Detoxification of reactive carbonyl species by glutathione transferase Tau isozymes.
500 Front. Plant Sci. 10: 487.
501 Mano, J., Biswas, M. S. and Sugimoto, K. (2019) Reactive carbonyl species: A missing link in
502 ROS signaling. Plants 8: 391.

503 Mueller, L. A., Zhang, P. and Rhee, S. Y. (2003) AraCyc: A biochemical pathway database for
504 Arabidopsis. Plant Physiol. 132: 453-460.

505 Nurbekova, Z., Srivastava, S., Standing, D., Kurmanbayeva, A., Bekturova, A., Soltabayeva,
506 A., Oshanova, D., Turečková, V., Strand, M., Biswas, M. S., Mano, J. and Sagi, M.
507 (2021) Arabidopsis aldehyde oxidase 3, known to oxidize abscisic aldehyde to ABA,
508 protects leaves from aldehyde toxicity. Plant J. 108: 1439-1455.
509 Phahom, T., Mano, J. (2023) Integration of multiple linear regression, principal component
510 analysis, and hierarchical cluster analysis for optimizing dried fingerroot
511 (*Boesenbergia rotunda*) extraction process. Journal of Applied Research on Medicinal
512 and Aromatic Plants 36: 100511.
513 Roach, T., Stöggl, W., Baur, T. and Kranner, I. (2018) Distress and eustress of reactive
514 electrophiles and relevance to light stress. Free Rad. Biol. Med., 122: 65-73.

515 Schauenstein, E., Esterbauer, H. and Zollner, H. (1977) Aldehyde in Biological Systems: Their
516 Natural Occurrence and Biological Activities. Pion, pp. 589–590.

517 Song, X., Lu, Y., Lu, Y. and Lv, L. (2021) Adduct formation of acrolein with cyanidin-*O*-
518 glucoside and its degradants/metabolites during thermal processing or in vivo after
519 consumption of red bayberry. J. Agric. Food Chem. 69: 13143-13154.

520 Spaas, J., Franssen, W. M. A., Keytsman, C., Blancquaert, L., Vanmierlo, T., Bogie, J., Broux,
521 B., Hellings, N., van Horssen, J., Posa, D. K., Hoetker, D., Baba, S. P., Derave, W. and
522 Eijnde, B. O. (2021) Carnosine quenches the reactive carbonyl acrolein in the central
523 nervous system and attenuates autoimmune neuroinflammation. J. Neuroinflam., 18:
524 255.

525 Srivastava, S., Brychkova, G., Yarmolinsky, D., Soltabayeva, A., Samani, T. and Sagi, M.
526 (2017) Aldehyde oxidase 4 plays a critical role in delaying silique senescence by
527 catalyzing aldehyde detoxification. Plant Physiol. 173: 1977–1997.

528 Stoll, A. and Seebeck, E. (1948) Über Alliin, die genuine Muttersubstanz des Knoblauchöls. 1.
529 Mitteilung über Allium-Substanzen. Helv. Chim. Acta 31: 189-210.

530 Sugimoto, K., Matsuoka, Y., Sakai, K., Fujiya, N., Fujii, H. and Mano, J. (2021) Catechins in
531 green tea powder (matcha) are heat-stable scavengers of acrolein, a lipid peroxide-
532 derived reactive carbonyl species. Food Chem. 355: 129403.

533 Sultana, M. S., Yamamoto, S.-I., Biswas, M. S., Sakurai, C., Isoai, H. and Mano, J. (2022)
534 Histidine-containing dipeptides mitigate salt stress in plants by scavenging reactive
535 carbonyl species. J. Agric. Food Chem. 70: 11169-11178.

536 Sultana, M. S., Sakurai, C., Biswas, M. S., Szabados, L. and Mano, J. (2024) Accumulation of
537 reactive carbonyl species in roots as the primary cause of salt stress-induced growth
538 retardation of *Arabidopsis thaliana*. Physiol. Plant. 176: e14198.

539 Sunkar, R., Bartels, D. and Kirch, H.-H. (2003) Overexpression of a stress-inducible
540 aldehyde dehydrogenase gene from *Arabidopsis thaliana* in transgenic plants
541 improves stress tolerance. Plant J. 35: 452–464,.

542 Tao, Z.-h., Li, C., Xu, X.-f. and Pan, Y.-j. (2019) Scavenging activity and mechanism study of
543 ferulic acid against reactive carbonyl species acrolein. J. Zhejiang Univ.-Science B 20:
544 868-876.

545 Ueda, Y., Kawajiri, H., Miyamura, N. and Miyajima, R. (1991) Content of some sulfur-
546 containing components and free amino acids in various strains of garlic. Nippon
547 Shokuhin Kogyo Gakkaishi 38: 429-434.

548 Uemura, T., Uchida, M., Nakamura, M., Shimekake, M., Sakamoto, A., Terui, Y., Higashi, K.,
549 Ishii, I., Kashiwagi, K. and Igarashi, K. (2023) A search for acrolein scavengers among
550 food components. Amino Acids 55: 509-518.

551 Wang, W., Qi, Y., Rocca, J. R., Sarnoski, P. J., Jia, A. and Gu, L. (2015) Scavenging of toxic
552 Acrolein by resveratrol and hesperetin and identification of adducts. J. Agric. Food
553 Chem. 63: 9488-9495.

554 Wible, R. S. and Sutter, T. R. (2017) Soft cysteine signaling network: the functional
555 significance of cysteine in protein function and the soft acids/bases thiol chemistry that
556 facilitates cysteine modification. Chem. Res. Toxicol. 30: 729-762.

557 Yamauchi, Y., Hasegawa, A., Taninaka, A., Mizutani, M. and Sugimoto, Y. (2011) NADPH-
558 dependent reductases involved in the detoxification of reactive carbonyls in plants. J.
559 Biol. Chem. 286: 6999–7009.

560 Yamauchi, Y., Hasegawa, A., Mizutani, M. and Sugimoto, Y. (2012) Chloroplastic NADPH-
561 dependent alkenal/one oxidoreductase contributes to the detoxification of reactive
562 carbonyls produced under oxidative stress. FEBS Lett. 586: 1208-1213.

563 Yamazaki, Y., Iwasaki, K., Mikami, M. and Yogihashi, A. (2011) Distribution of eleven
564 flavor precursors, *S*-alk(en)yl-L-cysteine derivatives in seven Allium vegetables. Food
565 Sci. Technol. Res. 17: 55-62.

566 Yin, L., Mano, J., Wang, S., Tsuji, W. and Tanaka, K. (2010) The involvement of lipid
567 peroxide-derived aldehydes in aluminum toxicity of tobacco roots. Plant Physiol. 152:
568 1406–1417.

569 Zhang, D., Jiang, X., Xiao, L., Lu, Y., Sang, S., Lv, L. and Dong, W. (2020) Mechanistic
570 studies of inhibition on acrolein by myricetin. Food Chem. 323: 126788.

571 Zhu, Q., Zheng, Z.-P., Cheng, K.-W., Wu, J.-J., Zhang, S., Tang, Y. S., Sze, K.-H., Chen, J.,
572 Chen, F. and Wang, M. (2009) Natural polyphenols as direct trapping agents of lipid
573 peroxidation-derived acrolein and 4-hydroxy-trans-2-nonenal. Chem. Res. Toxicol. 22:
574 1721-1727.

575 Zou, Z., Yin, Z., Ou, J., Zheng, J., Liu, F., Huang, C. and Ou, S. (2021) Identification of adducts
576 formed between acrolein and alanine or serine in fried potato crips and the cytotoxicity-
577 lowering effect of acrolein in three cell lines. Food Chem. 361: 130164.

578

579 **ACKNOWLEDGMENTS**

580 The authors would like to express their gratitude to Ryoma Oishi and Suzuka Monden for their
581 technical assistance and to Prof. Toshihiro Murafuji, Yamaguchi University, for discussion.

582

583 **FUNDING**

584 This work was supported by the Ministry of Agriculture, Forestry and Fisheries of Japan, by
585 KAKENHI Grants (nos. 17K19909 and 20H03278) from the Japan Society for the Promotion
586 of Science (to J. M.), and by Yamaguchi University Project for Formation of the Core Research

Project. This work resulted from the use of research equipment shared in the MEXT Project for promoting public utilization of advanced research infrastructure (Program for supporting the construction of core facilities) Grant Number JPMXS0440400022.

Conflict-of-Interest Declaration

The authors declare no conflicts of interest associated with this manuscript.

Declaration of generative AI and AI-assisted technologies in the writing process

During manuscript preparation, the authors used AI-based language tools (DeepL, ChatGPT, Google Gemini) solely for improving English grammar and readability. All scientific content was conceived, verified, and revised by the authors, who take full responsibility for the manuscript.

Deposition of a preprint

A preprint of this manuscript is deposited in the bioRxiv server.